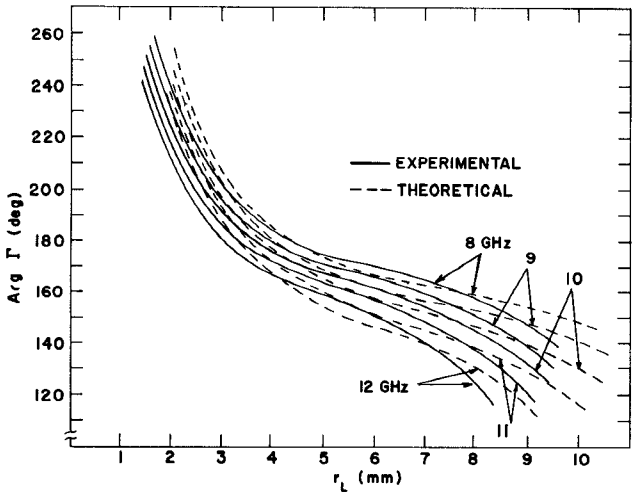

Fig. 4. Comparison of experimental and theoretical results for phase of the reflection coefficient of a half-moon element terminating a 50-Ω input microstrip transmission line ($\epsilon_r = 2.35$, $h = 250$ μm) as a function of radius with X-band frequency as a parameter.

specified reactance (approximately zero resistive component) at the center frequency as determined from information in Fig. 3. For example if a load with -24-Ω reactance at 10 GHz is required, this corresponds to $\Gamma = 1.0\angle -129°$ in a 50-Ω system. From Fig. 4 a half-moon circuit of radius $r_L = 1.9$ mm will have the desired reactance.

Also, in Fig. 4 it can be seen that for $2.7 < r_L < 4.3$ mm, the half-moon element is a broad-band RF short-circuit at point A with center frequency in X band. Note that since the half-moon circuit is a radial line element, the required r_L is less than a quarter-wavelength at the center frequency. The half-moon circuit can be used as a bias line for series-mounted active devices with the dc bias applied at point A through a microstrip transmission line of high characteristic impedance (> 100 Ω). Typically the arg (Γ) changes only $\pm 15°$, about the phase 180° at center frequency, over a 6-GHz bandwidth.

Alternative RF short-circuits have smaller bandwidth and larger area. For example, an RF short-circuit designed at 10 GHz using the half-moon element was compared with a low-impedance open-circuited quarter-wavelength microstrip stub. From Fig. 4, an outer radius $r_L = 3.65$ mm is required for the half-moon circuit (with inner radius $r_i = 0.38$ mm corresponding to a 50-Ω input microstrip line). For a meaningful comparison the characteristic impedance of the microstrip stub must be chosen carefully. A terminal characteristic impedance for the radial line can be defined as

$$Z_{0T}(kr) = \frac{h}{\alpha r} Z_0(kr) \tag{8}$$

from (4) and (7). Then the radial line stub will have an equivalent characteristic impedance defined as

$$Z_{eq} = \sqrt{Z_{0T}(kr_i) Z_{0T}(kr_L)}\ . \tag{9}$$

Since $Z_{0T}(kr_i) = 17.3$ Ω and $Z_{0T}(kr_L) = 5.1$ Ω, a microstrip stub having characteristic impedance $Z_0 = Z_{eq} = 9.4$ Ω was constructed for comparison purposes. The measured arg (Γ) for the 9.4-Ω open-circuited quarter-wavelength stub changed 29° over the band 7–13 GHz whereas the arg (Γ) for the half-moon element changed 22° over the same bandwidth. In addition to the wider bandwidth, the half-moon element has a smaller physical area (21 mm^2) than the low-impedance rectangular stub (28 mm^2).

It is usually advantageous for shunt-mounted active devices to be biased looking into an RF open-circuit. The broad-band RF short-circuit at point A in Fig. 2(b) can be transformed into an RF open-circuit at point B, with little sacrifice in bandwidth, by means of a quarter-wavelength microstrip line of high characteristic impedance. Again the dc bias should be applied at point A through another line of high characteristic impedance but of arbitrary length. Typically arg (Γ) at point B changed $\pm 18°$, about phase 0° at center frequency, over 4-GHz bandwidth. Two such configurations can be cascaded to improve bandwidth if necessary.

V. Conclusions

The half-moon radial line element displays broad-band reflection coefficient properties which make it a useful one-port microstrip circuit element. It is especially well suited for use in broad-band RF bias lines or tuning circuits for active devices. The analytical model presented for the half-moon circuit can be used for computer-aided circuit design.

Acknowledgment

The author would like to thank L. Besser of COMPACT Engineering for his helpful correspondence and also the Microwave Institute in Stockholm, Sweden, for providing the measurement facilities used during the course of this work.

References

[1] C. S. Aitchison *et al.*, "Lumped-circuit elements at microwave frequencies," *IEEE Trans. Microwave Theory Tech.*, vol. MTT-19, pp. 928–937, Dec. 1971.
[2] R. V. Garver, "360° varactor linear phase modulator," *IEEE Trans. Microwave Theory Tech.*, vol. MTT-17, pp. 137–147, Mar. 1969.
[3] I. Wolff and N. Knoppik, "Microstrip ring resonator and dispersion measurement on microstrip lines," *Electron. Lett.*, vol. 7, pp. 779–781, Dec. 30, 1971.
[4] S. Ramo, J. R. Whinnery, and T. Van Duzer, *Fields and Waves in Communication Electronics*. New York: Wiley, 1967, pp. 453–458.
[5] C. G. Montgomery, R. H. Dicke, and E. M. Purcell, *Principles of Microwave Circuits*, (MIT Rad. Lab. Series, no. 8). New York: McGraw-Hill, 1948.
[6] J. P. Vinding, "Radial line stubs as elements in stripline circuits," *NEREM Record*, pp. 108–109, 1967.
[7] J. P. Vinding, "Strip line electrical filter element," U. S. Patent 3 566 315, Feb. 1971.
[8] H. A. Wheeler, "Transmission-line properties of parallel strips separated by a dielectric sheet," *IEEE Trans. Microwave Theory Tech.*, vol. MTT-13, pp. 172–185, Mar. 1965.
[9] B. A. Syrett, "The use of the automatic network analyzer in the development and modelling of a novel broad-band bias line for X-band microstrip circuits," M. Eng. thesis, Carleton University, Ottawa, Canada, Jan. 1973.

Dispersion in n Coupled Microstrip Meanders

A. K. AGRAWAL

***Abstract*—A meander line consisting of an even (n), or odd ($n-1$), number of coupled microstrips has been analyzed for its dispersion and iterative impedance characteristics. In contrast with the unit cell approximation used by other authors, this method takes all the couplings into account and enables correct determination of stopband locations, which is**

Manuscript received October 23, 1979; revised March 19, 1980.
The author is with Panjab Engineering College, 323/15-A Chandigargh Pin 160016, India.

very important in the design of such slow-wave structures. Other periodic structures can also be analyzed by this method, and their possible future applications as filters, etc., can be predicted.

I. Introduction

Slow-wave structures, which consist of different types of spatially periodic media, occur in a variety of physical situations and are used in crossed-field amplifiers (CFA), and in the solid-state traveling wave amplifiers. An infinite array of coupled lines with connections at the alternate ends, thus forming a meander line (one form of slow-wave structure), has been analyzed for its dispersion and other characteristics with some approximations.

Jones and Bolljahn [1], and Libbey [2], have described the theory of the basic single-coupled pair of lines, but they did not take into account the variations of the even- and odd-mode-characteristic impedances Z_e and Z_o, and velocities of propagation V_e and V_o, with frequency f. Weiss [3], and Crampagne and Ahmadpanah [4], [5], have considered these variations, but analyzed a single unit cell embracing two lines only of the periodic medium and thus neglected the couplings between the unit cell and other lines. Moreover, the unit cell approximation cannot be used when the total number of lines is odd.

In this paper a microstrip meander line consisting of an even (n), and odd ($n-1$), number of lines has been analyzed for its dispersion θ, and iterative impedance Z_{it}, characteristics, taking the couplings into account. This enables correct prediction of stopband locations, which is very important for the design purposes.

II. Terminal Voltages

The structure to be analyzed is shown in Fig. 1. The constant current generators i_1 and i_2 for the even mode, and i_{2r-1} and i_{2r} for the odd mode, respectively, are assumed to energize the rth line ($r=2,3,\cdots,n$). The voltages on the rth and $(r-1)$th lines are of the form

$$\begin{aligned}
V_{r,1}^{e}(x) &= V_{r-1,1}^{e}(x) = -jZ_e i_1 \frac{\cos K_e(L-x)}{\sin K_e L}\\
V_{r,2r-1}^{o}(x) &= -V_{r-1,2r-1}^{o}(x) = -jZ_o i_{2r-1} \frac{\cos K_o(L-x)}{\sin K_o L}\\
V_{r,2}^{e}(x) &= V_{r-1,2}^{e}(x) = -jZ_e i_2 \frac{\cos K_e x}{\sin K_e L}\\
V_{r,2r}^{o}(x) &= -V_{r-1,2r}^{o}(x) = -jZ_o i_{2r} \frac{\cos K_o x}{\sin K_o L}
\end{aligned} \tag{1}$$

where $K_e=2\pi f/v_e$ and $K_o=2\pi f/v_o$ are the even- and odd-mode propagation constants, v_e and v_o are the velocities of the respective modes, and f is the frequency of excitation. The total voltages at the rth and $(r-1)$th terminals are

$$\begin{aligned}
V_r(x) &= V_{r,1}^{e}(x) + V_{r,2r-1}^{o}(x) + V_{r,2}^{e}(x)\\
&\quad + V_{r,2r}^{o}(x) + V_{r,2r+1}^{o}(x) + V_{r,2r+2}^{o}(x)\\
&= -jZ_e i_1 \frac{\cos K_e(L-x)}{\sin K_e L} - jZ_o i_{2r-1} \frac{\cos K_o(L-x)}{\sin K_o L}\\
&\quad - jZ_e i_2 \frac{\cos K_e x}{\sin K_e L} - jZ_o i_{2r} \frac{\cos K_o x}{\sin k_o L}\\
&\quad + jZ_o i_{2r+1} \frac{\cos K_o(L-x)}{\sin K_o L} + jZ_o i_{2r+2} \frac{\cos K_o x}{\sin K_o L}
\end{aligned}$$

and

$$\begin{aligned}
V_{r-1}(x) &= V_{r-1,1}^{e}(x) + V_{r-1,2r-1}^{o}(x) + V_{r-1,2}^{e}(x)\\
&\quad + V_{r-1,2r}^{o}(x) + V_{r-1,2r-3}^{o}(x) + V_{r-1,2r-2}^{o}(x)\\
&= -jZ_e i_1 \frac{\cos K_e(L-x)}{\sin K_e L} + jZ_o i_{2r-1} \frac{\cos K_o(L-x)}{\sin K_o L}\\
&\quad - jZ_e i_2 \frac{\cos K_e x}{\sin K_e L} + jZ_o i_{2r} \frac{\cos K_o x}{\sin K_o L}\\
&\quad - jZ_o i_{2r-3} \frac{\cos K_o(L-x)}{\sin K_o L} - jZ_o i_{2r-2} \frac{\cos K_o x}{\sin K_o L}.
\end{aligned} \tag{2}$$

The terminal voltages are obtained on substitution of $x=0$, and $x=L$ in (2).

III. Transmission Matrices

A. Number of Lines Even (n)

When the number of lines is even the output is taken from the $(2n-1)$th terminal, as shown in Fig. 1. The mode currents in terms of terminal currents are

$$\begin{aligned}
i_1 &= \frac{1}{n}\sum_{1}^{n} I_{2r-1}\\
i_{2r-1} &= \frac{r-1}{n}\sum_{r}^{n} I_{2r-1} - \frac{n-r+1}{n}\sum_{1}^{r-1} I_{2r-1}\\
i_2 &= \frac{1}{n}\sum_{r}^{n} I_{2r}\\
i_{2r} &= \frac{r-1}{n}\sum_{r}^{n} I_{2r} - \frac{n-r+1}{n}\sum_{1}^{r-1} I_{2r}
\end{aligned}$$

which on substituting the boundary conditions for the terminal currents become

$$\begin{aligned}
i_1 &= \frac{1}{n}(I_1 + I_{2n-1})\\
i_{2r-1} &= \begin{cases} \dfrac{r-1}{n} I_{2n-1} - \dfrac{n-r+1}{n} I_1, & r \text{ even } (2,4,\cdots,n)\\ \dfrac{r-1}{n}(I_{2r-1}+I_{2n-1}) - \dfrac{n-r+1}{n}(I_1+I_{2r-3}), & r \text{ odd } (3,5,\cdots,n-1) \end{cases}\\
i_2 &= 0\\
i_{2r} &= \begin{cases} I_{2r}, & r \text{ even } (2,4,\cdots,n)\\ 0, & r \text{ odd } (1,3,\cdots,n-1) \end{cases}.
\end{aligned} \tag{3}$$

When (3) is substituted into (2) and the boundary conditions for the terminal voltages are applied, the following $(n+1)\times(n+1)$ impedance matrix equation (for n lines) is obtained. The upper left partition of the impedance matrix has $(\frac{n}{2}+1)\times(\frac{n}{2}+1)$ terms, the lower right has $\frac{n}{2}\times\frac{n}{2}$ terms, and

$$\begin{aligned}
R &= \frac{(Z_e/Z_o)\cot K_e L \tan K_o L + n - 1}{n}\\
S &= \frac{(Z_e/Z_o)\cot K_e L \tan K_o L - 1}{n}
\end{aligned} \tag{4}$$

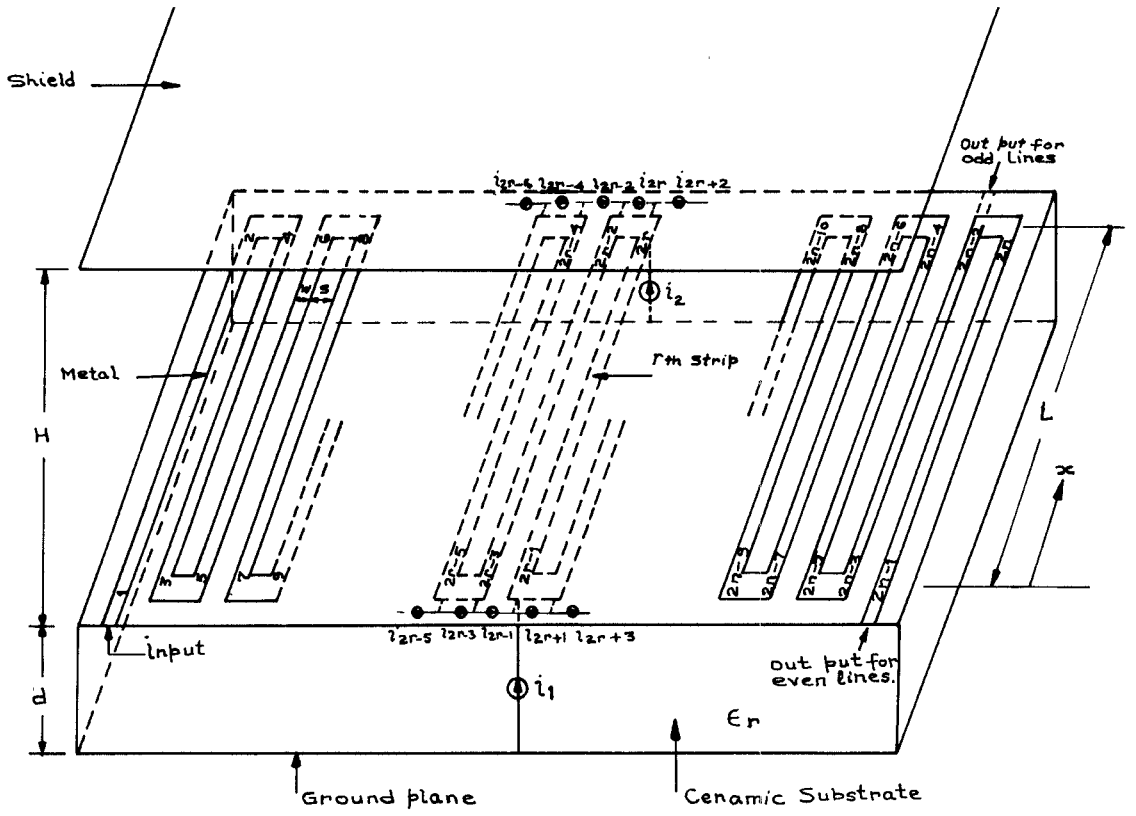

Fig. 1. An array of n coupled microstrip lines in meander form. ($W=0.8$ mm, $S=0.13$ mm, $d=1$ mm, $H=10$ cm, and $\epsilon_r=9.6$)

$$\begin{bmatrix} V_1 \\ 0 \\ 0 \\ \vdots \\ 0 \\ 0 \\ V_{2n-1} \\ 0 \\ 0 \\ 0 \\ \vdots \\ 0 \\ 0 \\ 0 \end{bmatrix} = \frac{-jZ_o}{\sin K_o L} \left[\begin{array}{ccccccc|ccccccc} RC & 0 & \cdots & & & & SC & -1 & 0 & \cdots & & & & 0 \\ 0 & 2C & 0 & \cdots & & & 0 & 1 & 1 & 0 & \cdots & & & 0 \\ 0 & 0 & 2C & 0 & \cdots & & 0 & 0 & 1 & 1 & 0 & \cdots & & 0 \\ \vdots & & & & & & & & & & & & & \vdots \\ 0 & \cdots & 0 & 2C & 0 & 0 & & 0 & \cdots & 0 & 1 & 1 & 0 & I_{2n-9} \\ 0 & \cdots & 0 & 0 & 2C & 0 & & 0 & \cdots & 0 & 0 & 1 & 1 & I_{2n-5} \\ SC & 0 & \cdots & & 0 & RC & & 0 & \cdots & & 0 & 0 & 1 & I_{2n-1} \\ \hline 1 & -1 & 0 & \cdots & & & 0 & -2C & 0 & \cdots & & & & 0 \\ 0 & -1 & -1 & 0 & \cdots & & 0 & 0 & -2C & 0 & \cdots & & & 0 \\ 0 & 0 & -1 & -1 & 0 & \cdots & 0 & 0 & 0 & -2C & 0 & \cdots & & 0 \\ \vdots & & & & & & & & & & & & & \vdots \\ 0 & \cdots & 0 & -1 & -1 & 0 & 0 & 0 & \cdots & 0 & -2C & 0 & 0 & I_{2n-8} \\ 0 & \cdots & 0 & 0 & -1 & -1 & 0 & 0 & \cdots & 0 & 0 & -2C & 0 & I_{2n-4} \\ 0 & \cdots & 0 & 0 & -1 & -1 & & 0 & \cdots & 0 & 0 & 0 & -2C & I_{2n} \end{array}\right] \begin{bmatrix} I_1 \\ I_3 \\ I_7 \\ \vdots \\ I_{2n-9} \\ I_{2n-5} \\ I_{2n-1} \\ I_4 \\ I_8 \\ I_{12} \\ \vdots \\ I_{2n-8} \\ I_{2n-4} \\ I_{2n} \end{bmatrix} \tag{5}$$

Here $C=\cos K_o L$.

B. Number of Lines Odd ($n-1$)

Referring to Fig. 1, for $(n-1)$ lines the output is taken at the $2n$th terminal. The mode currents in this case are given by

$x=0$

$$i_1=\frac{1}{n-1}\sum_{1}^{n-1} I_{2r-1}$$

$$i_{2r-1}=\sum_{r}^{n-1} I_{2r-1}-\frac{(n-r)}{(n-1)}\sum_{1}^{n-1} I_{2r-1}$$

$x=L$

$$i_2=\frac{1}{n-1}\sum_{1}^{n-1} I_{2r}$$

$$i_{2r}=\sum_{r}^{n-1} I_{2r}-\frac{(n-r)}{(n-1)}\sum_{1}^{n-1} I_{2r}.$$

When boundary conditions are substituted into the above equations, the mode currents become

$x=0$

$$i_1=\frac{I_1}{n-1}$$

$$i_{2r-1}=\begin{cases} -\dfrac{(n-r)}{(n-1)}I_1, & r \text{ even } (2,4,\cdots,n-2) \\ I_{2r-1}-\dfrac{(n-r)}{(n-1)}I_1, & r \text{ odd } (3,5,\cdots,n-1) \end{cases}$$

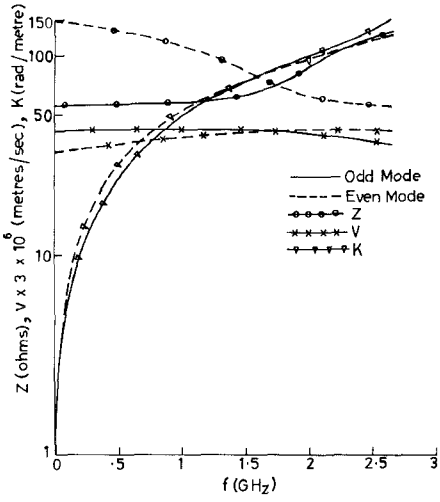

Fig. 2. The characteristic impedance, phase velocity, and phase shift constant of the unit cell versus frequency.

$x = L$

$$i_2 = \frac{I_{2n-2}}{n-1}$$

$$i_{2r} = \begin{cases} I_{2r} + \dfrac{(r-1)}{(n-1)} I_{2n-2}, & r \text{ even } (2,4,\cdots,n-2) \\ \dfrac{(r-1)}{(n-1)} I_{2n-2}, & r \text{ odd } (3,5,\cdots,n-1) \end{cases} \quad (6)$$

On substitution of (6) into (2) the following matrix equation (for $(n-1)$ lines) is obtained

$$\begin{bmatrix} V_1 \\ 0 \\ 0 \\ \vdots \\ 0 \\ 0 \\ 0 \\ \hline 0 \\ 0 \\ 0 \\ \vdots \\ 0 \\ 0 \\ V_{2n-2} \end{bmatrix} = \frac{-jZ_o}{\sin K_o L} \left[\begin{array}{ccccccc|ccccccc} UC, & 0, & \cdots & & & 0 & & 1, & 0, & \cdots & & 0, & V \\ 0, & -2C, & 0, & \cdots & & 0 & & -1, & -1, & 0, & \cdots & 0, & 0 \\ 0, & 0, & -2C, & 0, & \cdots & 0 & & 0, & -1, & -1, & 0, & \cdots & 0 \\ & & & & & & & & & & & & \\ 0, & \cdots & ,0, & -2C, & 0, & 0 & & 0, & \cdots & ,0, & -1, & -1, & 0 \\ 0, & \cdots & 0, & -2C, & 0 & & & 0, & \cdots & , & 0, & -1, & -1 \\ 0, & \cdots & 0, & -2C & & & & 0, & \cdots & 0, & -1, & -1 & \\ \hline 1, & 1, & 0, & \cdots & & 0 & & 2C, & 0, & \cdots & & 0 & \\ 0, & 1, & 1, & 0, & \cdots & 0 & & 0, & 2C, & 0, & \cdots & 0 & \\ 0, & 0, & 1, & 1, & 0, & 0 & & 0, & 0, & 2C, & 0, & 0 & \\ & & & & & & & & & & & & \\ 0, & \cdots & ,0, & 1, & 1, & 0 & & 0, & \cdots & , & 0, & 2C, & 0 \\ 0, & \cdots & , & 0, & 1, & 1 & & 0, & \cdots & , & 0, & 2C, & 0 \\ V, & 0, & \cdots & , & 0, & 1 & & 0, & \cdots & , & 0, & UC & \end{array}\right] \begin{bmatrix} I_1 \\ I_5 \\ I_9 \\ \vdots \\ I_{2n-11} \\ I_{2n-7} \\ I_{2n-3} \\ \hline I_2 \\ I_6 \\ I_{10} \\ \vdots \\ I_{2n-10} \\ I_{2n-6} \\ I_{2n-2} \end{bmatrix} \quad (7)$$

It should be noted in (7), that n is even,

$$U = \frac{\dfrac{Z_e}{Z_o} \cot K_e L \tan K_o L + n - 2}{n-1}$$

$$V = \frac{\dfrac{Z_e}{Z_o} \dfrac{\sin K_o L}{\sin K_e L} - 1}{n-1} \quad (8)$$

and

$$C = \cos K_o L.$$

IV. Dispersion Characteristics

A. Even Number of Lines

By inversion of the matrix in (5), the following 4-element admittance matrix between input and output terminals can be obtained

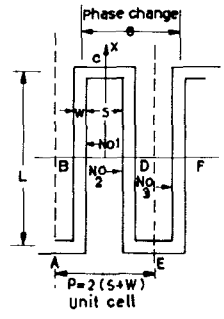

Fig. 3. A unit cell of the periodic array of meanders.

$$\begin{bmatrix} I_1 \\ I_{2n-1} \end{bmatrix} = \frac{j \sin K_o L}{Z_o} \begin{bmatrix} Y_{1,1} & Y_{1,n/2+1} \\ Y_{n/2+1,1} & Y_{n/2+1,n/2+1} \end{bmatrix} \begin{bmatrix} V_1 \\ V_{2n-1} \end{bmatrix}. \quad (9)$$

The iterative impedance Z_{it} and phase shift θ are obtained from (9), assuming zero attenuation, as

$$Z_{it} = \sqrt{\frac{Y_{n/2+1,n/2+1}}{Y_{1,1}} \cdot \frac{1}{\delta Y}}$$

$$\theta = \cos^{-1}\left(- \frac{\sqrt{Y_{1,1} \cdot Y_{n/2+1,n/2+1}}}{Y_{1,n/2+1}} \right) \quad (10)$$

where $\delta Y = Y_{1,1} \cdot Y_{n/2+1,n/2+1} - Y_{1,n/2+1} \cdot Y_{n/2+1,1}$.

B. Odd Number of Lines

The admittance matrix relating input and output terminal behavior is also determined by inversion of the matrix in (7) as follows:

$$\begin{bmatrix} I_1 \\ I_{2n-2} \end{bmatrix} = \frac{j \sin K_o L}{Z_o} \begin{bmatrix} Y_{1,1} & Y_{1,n} \\ Y_{n,1} & Y_{n,n} \end{bmatrix} \begin{bmatrix} V_1 \\ V_{2n-2} \end{bmatrix}. \quad (11)$$

Z_{it} and θ (assuming zero attenuation), become

$$Z_{it} = \sqrt{\frac{Y_{n,n}}{Y_{1,1}} \cdot \frac{1}{\delta Y}}$$

and

$$\theta = \cos^{-1}\left(- \frac{\sqrt{Y_{1,1} \cdot Y_{n,n}}}{Y_{1,n}} \right) \quad (12)$$

where $\delta Y = Y_{1,1} \cdot Y_{n,n} - Y_{1,n} \cdot Y_{n,1}$.

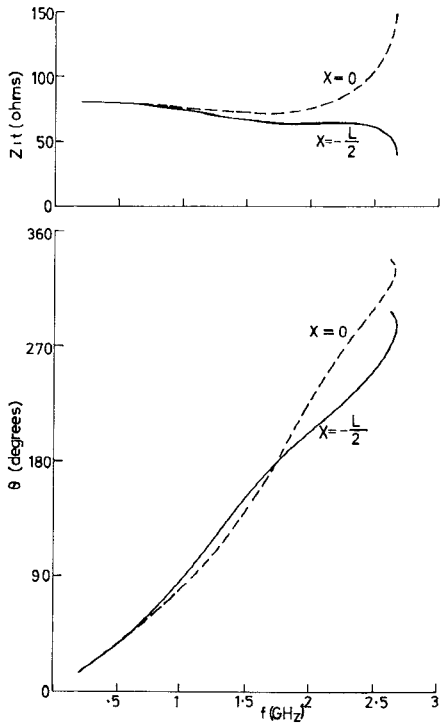

Fig. 4. The iterative impedance and phase shift versus frequency for the unit cell.

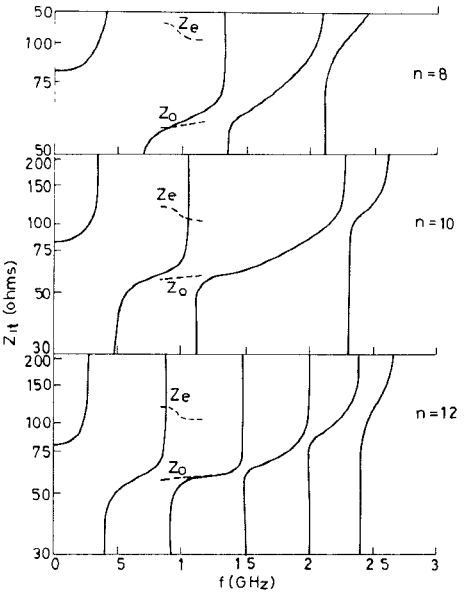

Fig. 5. The iterative impedance of an even number (n) of lines. Z_e and Z_o of one line-pair of the same configuration are also shown for comparison by dashed lines.

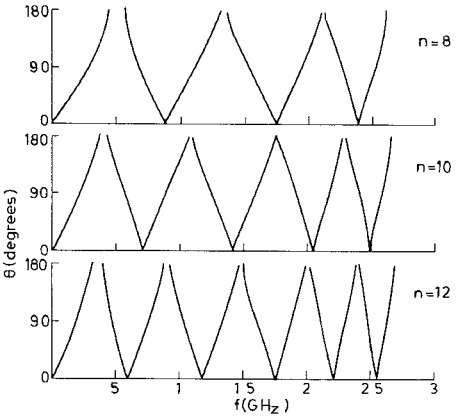

Fig. 6. The phase shift due to an even number (n) of lines.

V. Results

Computations involving inversion of the impedance matrices in (5) and (7) (for $n=2,4,\cdots,12$) were performed on the RCC DEC system 20 monitor, and the results are to be discussed.

A. Two Lines ($n=2$)

Before considering more than one coupled pair of lines, the calculated θ and Z_{it} curves for a unit cell were compared with those published by Crampagne and Ahmadpanah. Assuming the same line dimensions, and the same variation of Z_e, Z_o, V_e, and V_o with frequency as shown in Fig. 2, the data were found to be identical when the input and output ports of the unit cell were chosen at $x=0$. The unit cell so formed is shown as meander *BCDEF* in Fig. 3. Fig. 2 also shows the calculated curves of the even- and odd-mode phase shift constants K_e and K_o, (assuming zero attenuation) versus frequency.

Fig. 4 shows the calculated Z_{it}, and θ curves for the meander *BCDEF* (dashed lines), which do resemble those previously published [5]. On the other hand Fig. 4 also shows the calculated curves for the meander *ABCDE* (solid lines), whose input and output ports are located at $x=-\frac{L}{2}$. These curves differ from these previously published. Z_{it} and θ, therefore, are not independent of x, the location of the input and output ports of the unit cell. This result contradicts the assumption of Weiss [3], and Crampagne and Ahmadpanah [4], for according to them

$$V_3(x)=V_1(x)e^{j\theta} \tag{13}$$

where θ has been assumed to be same for all x. The assumption in (13) is invalid for the following reason.

The meander *BCDEF* consists of a series connection of *BCD* and *DEF* which are uncoupled. Therefore, the total phase change θ from B to F is equal to 2ϕ where ϕ is the calculated phase shift for the meander *BCD* (or *DEF*) of length $L/2$. Also, Z_{it} for *BCDEF* is equal to that for *BCD* (or *DEF*). In fact, the dashed curves in Fig. 4 which compare favorable with the published ones are plots of Z_{it}, and 2ϕ, for a meander of line length $L/2$. They must obviously differ from the solid curves which are calculated for the meander *ABCDE* of length L.

B. Number of Lines Even (n)

The output terminals for the even-line case are identified in Fig. 1. The calculated curves of Z_{it}, and θ, versus frequency are shown in Figs. 5 and 6 for $n=8$, 10, and 12. It is seen that the odd pairs ($n=2,6,10,\cdots$) of coupled lines have broader and more uniform passbands than even pairs ($n=4,8,12\cdots$). As the number of line pairs is increased, more stopbands appear and they shift towards lower frequencies. The number of stopbands is more for even pairs of coupled lines, but the phase changes at a comparatively slow rate.

C. Number of Lines Odd ($n-1$)

The input and output terminals for the odd-line case also indicated in Fig. 1. Figs. 7 and 8 show the variation of calculated

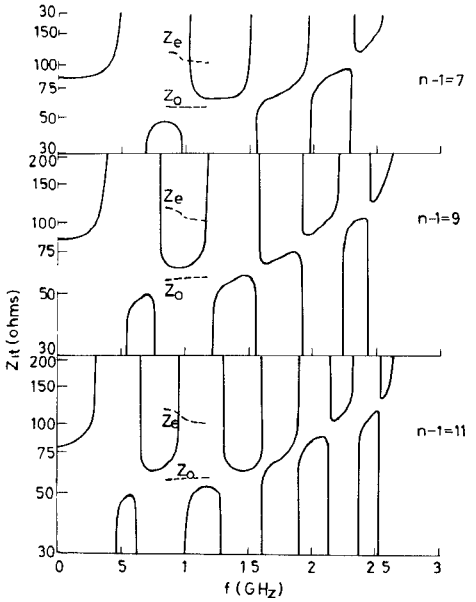

Fig. 7. The iterative impedance of an odd number $(n-1)$ of lines. Z_e and Z_o of one line-pair of the same configuration are also shown for comparison by dashed lines.

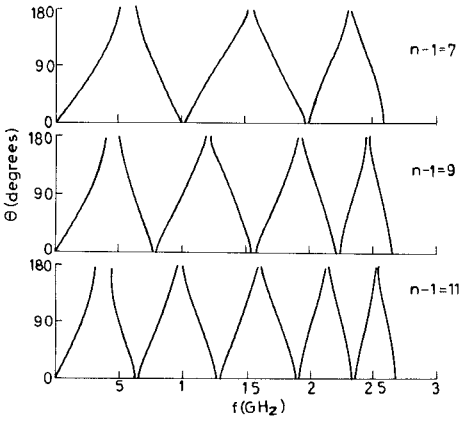

Fig. 8. The phase shift due to an odd number $(n-1)$ of lines.

Z_{it} and θ with frequency for 7, 9, and 11 lines. Around 17.5 GHz, all the curves have a passband; however, the Z_{it} characteristics for $3,7,11,\cdots$ lines differ markedly from those for $5,9,\cdots$ lines. In some passbands Z_{it} is nearly constant and phase shift is linear with frequency. With an increase in the number of lines, more stopbands appear and shift towards lower frequencies.

VI. Conclusion

Iterative impedance Z_{it}, and phase shift θ, (assuming negligible attenuation) have been calculated for even (8, 10, and 12), and odd (7, 9, and 11) coupled lines, and their variations with frequency have been compared. When all possible couplings are taken into account, it was found that the unit cell approximation is inadequate. The stopbands increase in number, become narrower, and shift towards lower frequencies as the number of lines is increased. For even pairs of lines, the number of stopbands increases and the phase changes at a slower rate when compared to the case of odd-pairs of lines. When the number of lines is odd, there is a clear difference between the Z_{it} curves for the groups of 3,7,11 lines and 5,9 lines. All the curves have a passband around 17.5 GHz. In some passbands, Z_{it} is uniform and θ is linear with frequency.

This method can be used for other periodic structures as well, e.g., interdigital line, etc., and enables determination of precise locations of stopbands.

Acknowledgment

The author wishes to express his thanks to Dr. K. N. Laxminarayan of the Physics Department, Panjab University, Chandigarh, India, and to Dr. Bharathi Bhatt, Centre for Applied Research in Electronics, Indian Institute of Technology, Delhi, India, for their valuable suggestions.

References

[1] E. M. T. Jones and J. T. Bolljahn, "Coupled-Strip-Transmission-Line Filters and Directional Couplers," *IRE Trans. Microwave Theory Tech.*, vol. MTT-4, pp. 75–81, Apr. 1956.

[2] W. M. Libbey, "Characteristics of a microstrip two-meander ferrite phase shifter," *IEEE Trans. Microwave Theory Tech.*, vol. MTT-21, pp. 483–487, July 1973.

[3] J. A. Weiss, "Dispersion and field analysis of a microstrip meander-line slow-wave structure, "*IEEE Trans. Microwave Theory Tech.*, vol. MTT-22, pp. 1194–1201, Dec. 1974.

[4] R. Crampagne and M. Ahmadpanah, "Meander and interdigital lines as periodic slow-wave structures. Part I. Characteristics of waves propagating along an infinite array," *Int. J. Electron.*, vol. 43, no. 1, pp. 19–32, July 1977.

[5] R. Crampagne and M. Ahmadpanah, "Meander and interdigital lines as periodic slow-wave structures. Part II. Applications to slow-wave structures." *Int. J. Electron.*, vol. 43, no. 1, pp. 33–39, July 1977.

The Bandwidth of Image Guide

RICHARD. J. COLLIER AND ROBIN D. BIRCH

***Abstract*—The various parameters involved in the bandwidth of image guide are discussed, viz., the aspect ratio and dielectric constant. Three definitions of bandwidth are given involving dispersion, wave-guiding properties and variation of characteristic impedance with velocity. Theoretical values of these definitions are given and the paper concludes with a discussion about their relative importance.**

I. Introduction

A large amount of work is being carried out into the uses of image line. At frequencies where better known wave guiding structures experience difficulties, by suitable choice of parameters, image lines can be made which are less susceptible to many of these problems. This work has been both theoretical [1]–[3], [10] and practical [4], [5] but little consideration has been paid to what actually are the practical constraints limiting the bandwidth available to image line. Without due consideration, it might appear that since the fundamental mode exists down to zero hertz the bandwidth is purely and simply the cutoff frequency of the next higher order mode. This is far from the case and this paper will discuss the major problems limiting the bandwidth. Topics such as dispersion, wave guiding properties and radiation will be dealt with, along with a discussion as to the usable upper frequency limit.

Manuscript received December 28, 1979; revised March 19, 1980.

The authors are with the Electronics Laboratories, University of Kent at Canterbury, Canterbury, Kent CT2 7NT, England.